Chemical Science

Accepted Manuscript

This article can be cited before page numbers have been issued, to do this please use: I. S. Yadav, A. Z. Alsaleh, R. Misra and F. D'Souza, *Chem. Sci.*, 2021, DOI: 10.1039/D0SC04648E.

ROYAL SOCIETY OF CHEMISTRY

rsc.li/chemical-science

View Article Online
DOI: 10.1039/D0SC04648E

Charge Stabilization via Electron Exchange: Excited Charge Separation in Symmetric, Central Triphenylamine Derived, Dimethylaminophenyl-Tetracyanobutadiene Donor-Acceptor Conjugates

Indresh S. Yadav,[a‡] Ajyal Z. Alsaleh,[b‡] Rajneesh Misra[a] and Francis D'Souza[b*]*

[a]*Department of Chemistry, Indian Institute of Technology, Indore 453552, India. E-mail: rajneeshmisra@iiti.ac.in*

[b]*Department of Chemistry, University of North Texas, 1155 Union Circle, #305070, Denton, TX 76203-5017, USA, E-mail: Francis.DSouza@UNT.edu*

[‡]*Equal contribution*

(Abstract). Photoinduced charge separation in donor-acceptor conjugates play a pivotal role in technology breakthroughs, especially in the areas of efficient conversion of solar energy into electrical energy and fuels. Extending the lifetime of the charge separated species is a necessity for their practical utilization, and this is often achieved by following the mechanism of natural photosynthesis where the process of electron/hole migration occurs distantly separating the radical ion-pairs. Here, we hypothesize and demonstrate a new mechanism to stabilize the charge separated states via the process of electron exchange among the different acceptor entities in multimodular donor-acceptor conjugates. For this, star-shaped, central triphenylamine derived, dimethylamine-tetracyanobutadiene conjugates have been newly designed and characterized. Electron exchange was witnessed upon electroreduction in conjugates having multiple numbers of electron acceptors. Using ultrafast spectroscopy, occurrence of excited state charge separation, and the effect of electron exchange in prolonging the lifetime of charge separated states in the conjugates having multiple acceptors has been successfully demonstrated. This work constitutes the first example of stabilizing charge-separated states via the process of electron exchange.

View Article Online
DOI: 10.1039/D0SC04648E

Introduction

Excited state charge transfer in donor-acceptor conjugates is one of the widely investigated topics in recent years due to their usage in building energy harvesting photonics devices.[1-19] Understanding the principles governing the kinetics of charge transfer and separation, securing high charge separation quantum yields, avoiding large energy losses, and prolonging the lifetime of the radical ion-pairs by molecular engineering of the conjugates have been the main focus of these studies.[1-12] In simple donor-acceptor conjugates, charge separation from the excited singlet state of the donor or acceptor can store the greatest amount of energy, however, since the process originates from the singlet excited state, the charge separated states are generally short-lived. In natural photosynthesis, lifetime of charge separation is prolonged by subsequent electron transfer to secondary acceptors.[20-22] This method of charge stabilization, optimizes the quantum yields but comes at the cost of lowering the overall efficiency due to the energy losses encountered during secondary electron transfer steps. Alternate approaches including electron/hole delocalization in conjugates having closely interacting multiple donor or acceptor entities,[23-24] and utilization of high energy triplet sensitizers to promote charge transfer from long-lived triplet excited states to prolong lifetime of charge separated states[25-26] have also been proven to work.

In recent years, the design and synthesis of π-conjugated symmetrical and unsymmetrical donor-acceptor chromophores have been extensively investigated due to their potential applications in organic photovoltaics,[27-30] molecular electronics[31] and bioimaging.[32] The star-shaped π-conjugated molecular systems exhibit many advantages over linear conjugated molecular systems including excellent solubility and lesser aggregation.[33] Tuning of electronic and photonic properties of these systems can be achieved by modulating the design of donor or acceptor units and connecting π-spacer unit.[34-36] The small organic π-conjugated donor-acceptor systems exhibit low band gap, intense absorption, and strong intramolecular interactions.[37-38] In several of these studies, triphenylamine, a classical nonplanar propeller shaped optoelectronic molecule, has been extensively used; extending their applications for developing field effect transistors, sensors, and solid state fluorescent and smart fluorescent materials.[39-40]

View Article Online
DOI: 10.1039/D0SC04648E

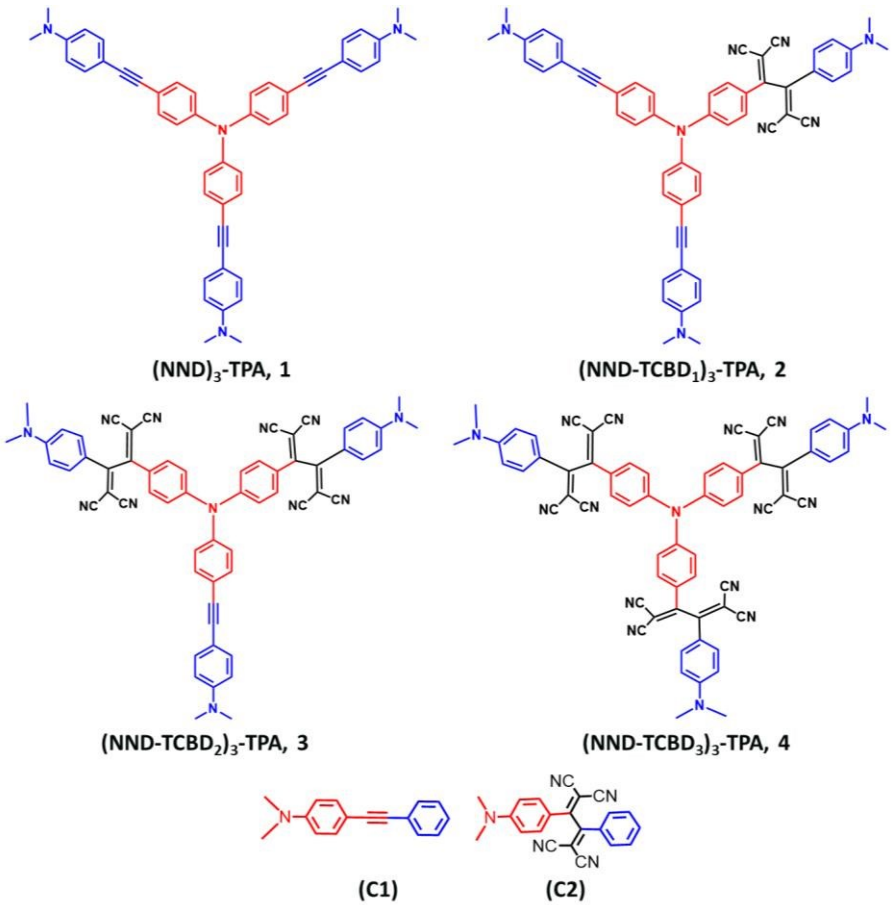

Chart 1. Structure and abbreviation of star-shaped, central triphenylamine derived, dimethylamine-tetracyanobutadiene conjugates, **1-4** and the control compounds, **C1-C2** newly designed, synthesized to demonstrate charge stabilization via electron exchange in the present study.

Tetracyanoethylene (TCNE) is a strong electron acceptor due to presence of four cyano groups, undergoes [2+2] cycloaddition reaction with electron rich alkynes to form cyclobutene rings followed by retroelectrocyclization reaction to give 1,1,4,4-tetracyanobutadiene (TCBD) derivatives.[41] The donor-acceptor systems containing TCBD acceptor are potential candidates for organic photovoltaics and non-linear optics due to strong intramolecular charge transfer (ICT) and lower HOMO-LUMO gaps.[42-48] Photochemical behavior of few donor-TCBD derived systems have been reported in literature.[49-56] Although with high quantum yields, due to close proximity between the donor and acceptor entities, ultrafast charge separation and recombination was observed in these systems. That is, no charge stabilization could be accomplished. In this regard, developing higher analogs of donor-TDCB bearing systems that would exhibit novel

View Article Online
DOI: 10.1039/D0SC04648E

photochemical properties including charge stabilization have been scarce due to the associated synthetic challenges. A recent example involves C_3-symmetric central truxene-derived phenothiazine-TCBD and its expanded molecular systems.[54] Although elegant, the central truxene made exclusively of saturated carbons played no role in stabilizing the charge separated states.

In the present study, we hypothesize that by choosing a redox/photoactive central unit instead of truxene, we could modulate the properties that would lead to novel redox- and photochemical discoveries. With this in mind, we have newly designed and synthesized star-shaped symmetric compound $(NND)_3$-TPA, **1** and their TCBD functionalized symmetric and unsymmetric derivatives $(NND\text{-}TCBD_{1\text{-}3})_3$-TPA, **2–4** (see Chart 1 for structures; NND = N,N-dimethylaminophenyl, TPA = triphenylamine and TCBD = 1,1,4,4-tetracyanobutadiene). These novel systems show strong intramolecular charge transfer (ICT) with lowered HOMO-LUMO gaps. Further, upon electroreduction of NND-TCBD entities in compounds **3** and **4** containing two and three NND-TCBD entities, electron exchange among the NND-TCBD was witnessed. Femtosecond transient absorption studies revealed occurrence of ultrafast charge transfer processes in these systems. Importantly, charge stabilization in **3** and **4** was witnessed as a consequence of electron exchange. These unpresented new findings provide a new mechanism of stabilizing the charge separated states via electron exchange in multi-modular donor-acceptor conjugates.

Results and Discussion

Scheme 1 shows the developed synthetic scheme for compounds **1-4** and their controls. Briefly, the symmetric $(NND)_3$-TPA, **1** was synthesized in 60% yield by the Pd-catalyzed Sonogashira cross coupling of tris-(4-iodo-phenyl)-amine and 4-ethynyl-*N*,*N*-dimethylaniline in degassed THF:TEA (1:1) under argon atmosphere, in the presence of $Pd(PPh_3)_4$ and CuI. Next, $(NND\text{-}TCBD_{1\text{-}3})_3$-TPA, **2–4** were synthesized *via* [2+2] cycloaddition-retroelectrocyclization reaction with the strong electron acceptor TCNE. The reaction of **1** with one equivalent of TCNE in DCM at room temperature for 4 h resulted in an exclusive mono TCBD bearing $(NND\text{-}TCBD_1)_3$-TPA, **2** in 63% yield. Similarly, the reaction of **1** with two equivalent of TCNE in DCM solvent at 40 ^oC for 12 h resulted in $(NND\text{-}TCBD_2)_3$-TPA, **3** in 65% yield, whereas upon increasing the reaction temperature to 80 ^oC in DCE solvent for 24 h using four equivalent of TCNE with **1**, resulted in symmetrical $(NND\text{-}TCBD_3)_3$-TPA, **4** in 70% yield. The control compound **C1** was

View Article Online
DOI: 10.1039/D0SC04648E

synthesized by the Pd-catalyzed Sonogashira cross-coupling reaction of 4-ethynyl-*N*,*N*-dimethylaniline and iodobenzene in 60% yield. The acetylene linked control compound **C1** further subjected to [2+2] cycloaddition-retro-electrocyclization reaction with one equivalent of TCNE at room temperature for 8 h, which resulted in TCBD substituted control compound **C2** in 82% yield. The newly synthesized compounds were purified over silica gel (100-200 mesh) column chromatography using Hexane:DCM as solvent and fully characterized by ^{1}H, ^{13}C NMR and high-resolution mass spectroscopy (HRMS) techniques (see SI for spectral details, Figures S1 – S18).

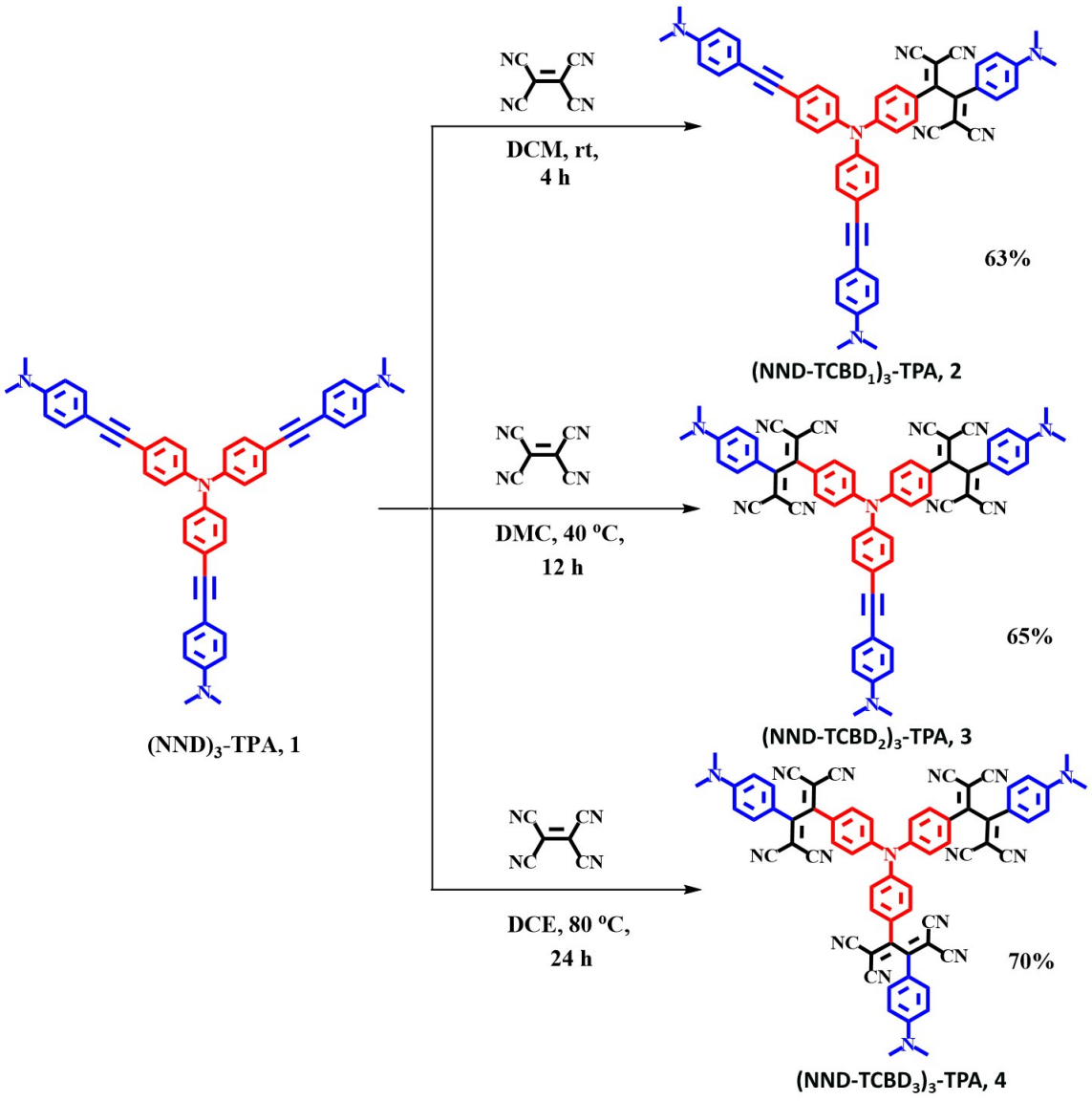

Scheme 1. Synthetic scheme of compounds **(NND)$_3$-TPA, 1** and **(NND-TCBD$_{1\text{-}3}$)$_3$-TPA, 2–4.**

View Article Online
DOI: 10.1039/D0SC04648E

Absorption spectrum of the investigated compounds is shown in Figure 1a. Control **C1**, having only a NND entity without either TPA or TCBD entities revealed an absorption band at 342 nm. In case of control **C2**, having an electron acceptor, TCBD next to the electron donor, NND entity, promoted charge transfer interactions between them. Consequently, two peaks, the first one at 315 and a second broad peak corresponding to charge transfer absorption at 478 nm, was observed. For compound **1**, having a central TPA and three terminal NND entities revealed a single absorption peak at 386 nm. As predicted, no charge transfer type peak was present. However, in the case of compounds **2-4**, having one, two and three TCBD entities between the NND and TPA entities, the expected charge transfer peak in the 478-484 nm region was possible to witness. In addition, a UV peak at 372 nm for **2**, 350 nm for **3** and, <300 nm for **4**, respectively, was also observed. Intensity of the charge transfer band increased with increasing the number of TCBD entities. Due to spectral similarities between **C2** and compounds **2-4**, and enhaneced absorption of the charge transfer band with increase in TDCB, it was possible to conclude that the origin of the charge transfer band is primarily due to interaction between NND and TCBD entities with lesser contributions from TPA interaction with TCBD. Optical data is summarized in Table 1.

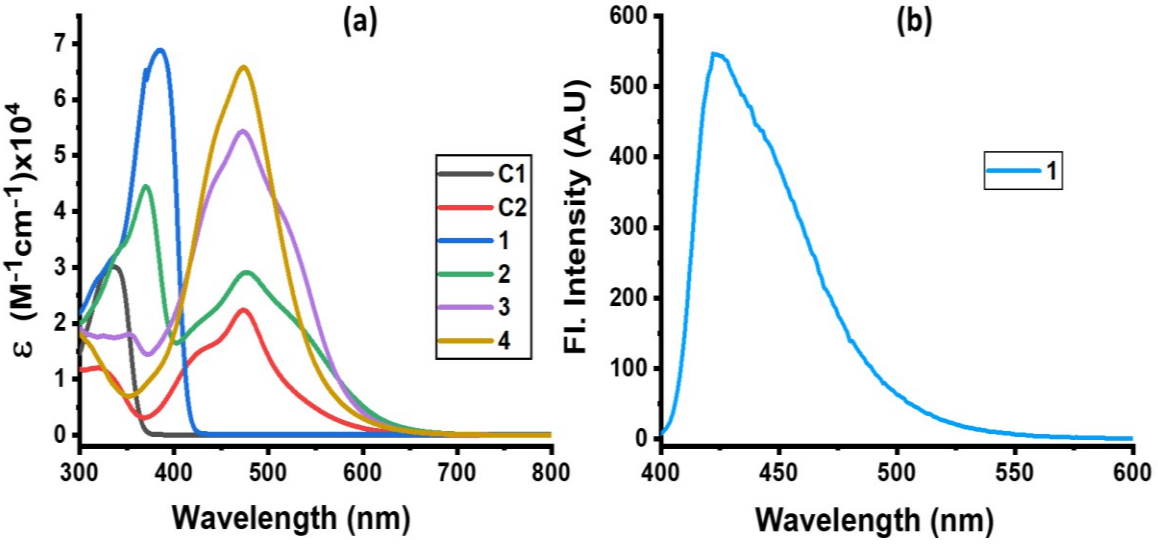

Figure 1. (a) Absorption and (b) fluorescence spectra of indicated compounds in DCB. Compound **1** was excited at 386 nm. No measurable emission was observed for compounds **2-4** upon exciting the samples either at the locally excited or charge transfer absorption peak positions.

View Article Online
DOI: 10.1039/D0SC04648E

Table 1. Absorption and fluorescence, redox potentials (V vs. Ag/AgCl), and free-energy changes for charge recombination (CR), charge separation (CS) and charge transfer (CT) for the investigated central triphenylamine derived, dimethylamine-tetracyanobutadiene conjugates in DCB.

System	λ_{max}, nm	E (10^5 M^{-1} cm^{-1})	λ_{em}, nm	Red-2 TCBD	Red-1 TCBD	Ox-1 TPA	Ox-2 NND	Ox-3 NND	$-\Delta G_{CR}$	$-\Delta G_{CS}$	$-\Delta G_{CT}$
C1	337	2.99		--	--	--	0.96	--	--	--	--
C2	327 473	1.16 2.23		-0.73	-0.39	--	1.43	--	--	--	--
1	384	6.89	420	--	--	0.80	1.15	--	--	--	--
2	372 477	4.40 2.91	419	-0.69	-0.43	0.88	1.30	1.45	1.11	1.85	2.56
3	354 472	1.80 5.43	418	-0.73	-0.33[a] -0.48	0.96	1.20	1.50	1.01	1.95	2.59
4	316 476	1.63 6.56	417	-0.70	-0.30[a] -0.40	1.35	1.63	--	1.35	1.61	2.59

[a]-split peak

Among the investigated compounds, only compound **1** revealed fluorescence emission as shown in Figure 1b. A broad peak with maxima at 420 nm and spectrum spanning the 400-575 nm range was observed (estimated quantum yield = 0.43). Lifetime from single photon counting technique revealed a monoexponential decay with a lifetime of 1.16 ns. For compounds **2-4**, having 1-3 numbers of strong electron acceptor TCBD entities, no measurable emission, either at the locally excited or charge transfer band positions, was observed; perhaps such emission were too weak to detect. In any case, the strong quenching observed in the case of compounds **2-4** suggest occurrence of excited state events such as energy or electron transfer in the highly interacting push-pull conjugates.

Next, in order to seek possible intramolecular interactions among the NND-TCBD entities via central TPA in compounds **3** and **4**, electrochemical studies using differential pulse (DPV) and cyclic voltammetry (CV) were performed in DCB containing 0.1 M (TBA)ClO_4. The site of electron transfer was arrived from control **C1** and **C2** and remainder of compounds, and is summarized in Table 1 and representative voltammograms are shown in Figure 2. Complete CVs

View Article Online
DOI: 10.1039/D0SC04648E

are shown in Figure S19 in SI.

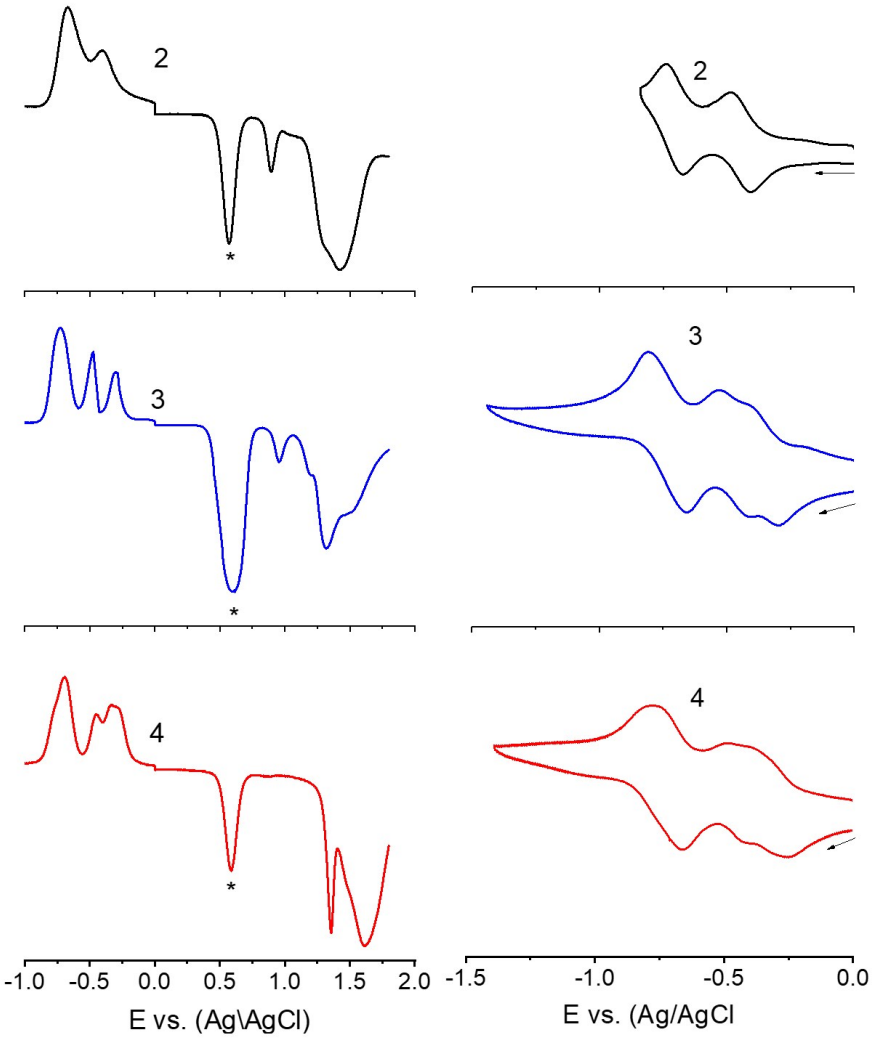

Figure 2. DPVs (left panel) and CVs (right panel) of indicated compounds in DCB containing 0.1 M $(TBA)ClO_4$. For DPV: scan rate = 5 mV/s, pulse width = 0.25 s, pulse height = 0.025 V. For CV: scan rate = 100 mV/s. The '*' in left panel represents oxidation peak of ferrocene used as internal standard. Note: the first reduction corresponding to TCBD in **3** and **4** is a split wave (see text for details).

Key observations from electrochemical studies involved: (i) The first oxidation of **C1** located at 0.96 V vs. Ag/AgCl was anodically shifted to 1.43 V in **C2** due the presence of electron deficient TCBD. The TCBD reductions, all one-electron reversible, were located at -0.39 and -0.73 V. (ii) Compound **1** revealed two oxidations, the first one at 0.80 V and a second one at 1.15 V. From the peak currents and by comparison with oxidation potential of **C1**, the first oxidation to TPA and the second one to NND entities was possible to arrive. (iii) In the case of compound

View Article Online
DOI: 10.1039/D0SC04648E

2, having a single NND-TCBD entity, the TPA oxidation was shifted to 0.88 V while the NND oxidations were split and appeared at 1.30 and 1.45 V owing to the presence of two types of NNDs (one linked to TCBD and another without TCBD). The TCBD reductions were located at -0.43 and -0.69 V. (iv) Introduction of a second TCBD entity in **3** and a third one in **4** revealed additional interesting features. As predicted, oxidation peaks revealed further anodic shift especially for TPA oxidation. Interestingly, the first reduction of TCBD in both compounds **3** and **4** were found to be

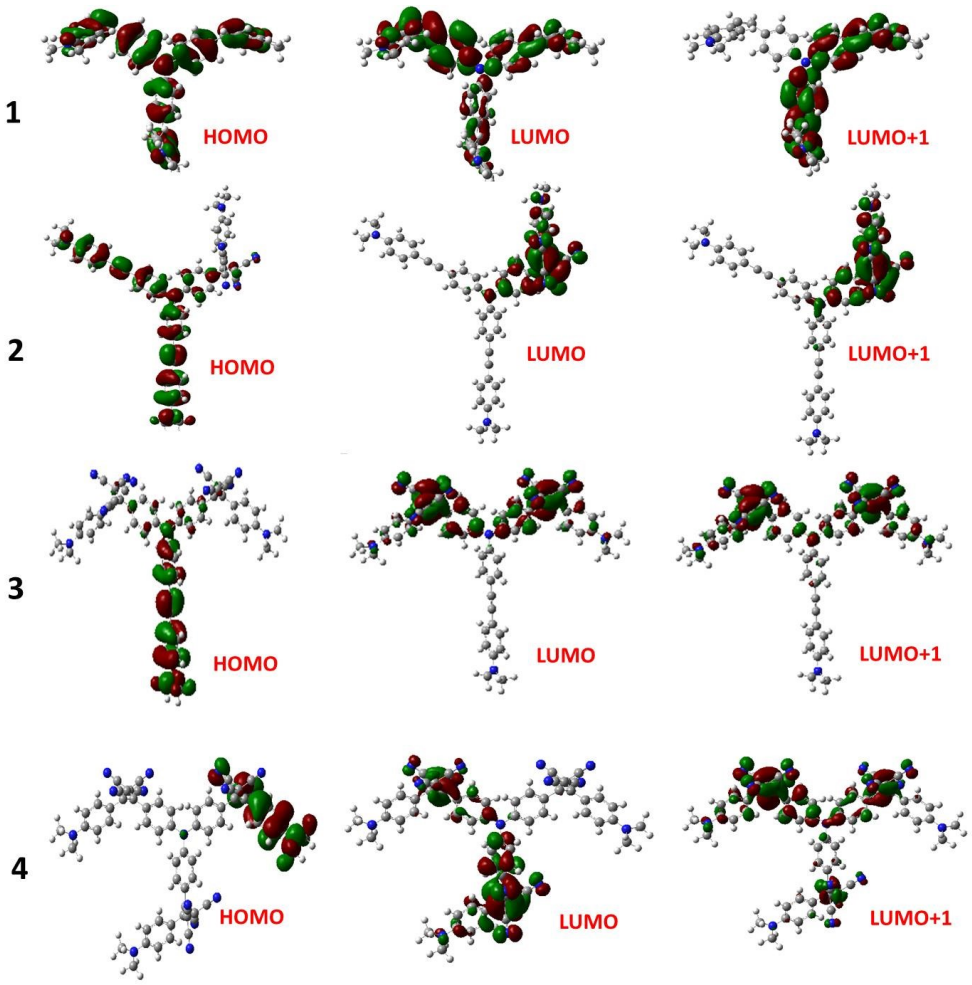

Figure 3. Frontier HOMO, LUMO and LUMO+1 of investigated compounds from the B3LYP/6-31G** optimized structures (see SI for coordinates of computed structures).

split waves. The split reduction peaks for **3** were located at -0.33 and -0.48 V, that is, a 140 mV potential difference while for **4**, the split peaks were located at -0.30 and -0.40 V, that is, about 100 mV potential difference. The second reduction of TCBD in both **3** and **4** were one-electron

View Article Online
DOI: 10.1039/D0SC04648E

reductions without noticeable splitting. The splitting of first reduction show electron exchange among the NND-TCBD entities in **3** and **4** via the central TPA entity.

The electron exchange between the NND-TCBD entities upon first electroreduction of compounds **3** and **4** motivated us to perform computational studies to probe their electronic structures. Compounds **1-4** were fully optimized on a Born-Oppenheimer potential energy surface at the B3LYP/6-31G* level calculations.[57] The generated frontier orbitals on the optimized structures are shown in Figure 3. The C_3 type symmetry originating from the central TPA entity was obvious in all these compounds. In the case of **1**, the HOMO was distributed evenly on the entire molecule while the LUMO coefficient was slightly more on one of the arms. In the case of **2**, the HOMO was localized NND-TPA arms while the LUMOs were on the TCBD entity with some contributions extending into the NND and TPA entities. The energy difference between the two LUMOs was 0.0211 hartrees. In the case of compound **3**, the HOMO occupied only the NND-TPA arm while the LUMOs occupied the two NND-TCBD with almost even distribution. The energy difference between the two LUMOs was 0.00527 hartrees. This situation was also true for compound **4**, where the LUMO was distributed over two NND-TCBD entities while the LUMO+1 had contribution on all three NND-TDBD entities. The energy difference between the LUMOs was 0.0047 hartrees. Splitting of the first reduction peak due to electron exchange in the case of compounds **3** and **4** can now be attributed to energetically closely spaced LUMOs.

One of the approaches to visualize the spectrum of charge separation products is by performing spectroelectrochemical studies followed by spectral interpretation. Here, by applying appropriate potentials corresponding to oxidation or reduction, spectrum of the radical cation and radical anion can be generated. Subsequently, the average of the radical cation and radical anion spectrum will be digitally generated and subtracted from the spectrum of the neutral compound. This represents the differential absorption spectrum of the charge separation product. Positive peaks represent transitions associated with the electron transfer product while negative peaks represent depletion of the absorption of the neutral compound.[54] We have used this approach in the present study as shown in Figure 4a-c. Spectral changes associated during first oxidation of **3** is shown in Figure 4a. A new peak during the process of oxidation was observed at 662 nm. The spectral changes were minimal in the visible region as the main 478 nm peak was due to NND-TDCB charge transfer transition whereas the oxidation was on the TPA entity (*vide supra*), ascertaining the earlier discussed site of electron transfer. On the contrary, the spectral changes

View Article Online
DOI: 10.1039/D0SC04648E

during first reduction (Figure 4b) revealed drastic decrease in intensity of the charge transfer band with broad positive spectral features in the 600-800 nm range. It may be mentioned here that during both oxidation and reduction, now new peaks beyond 800 nm was observed. The spectrum generated for the charge transfer product using the above described procedure is shown in Figure 4c. Such spectrum revealed a positive peak at 670 nm and depleted peak at 478 nm. Witnessing such a spectrum in transient absorption spectral studies would provide direct proof of charge transfer in these donor-acceptor conjugates. Similar spectra were derived for compounds **2** and **4** (see Figure S20 in SI).

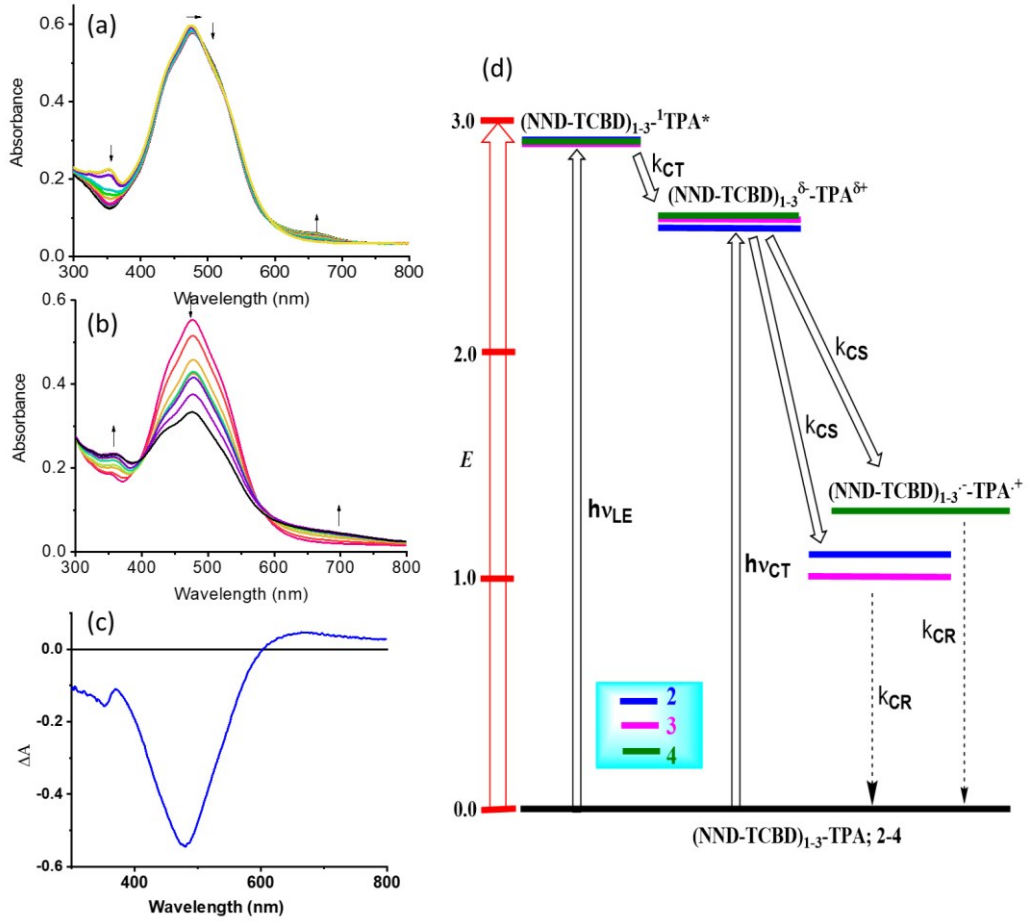

Figure 4. Spectral changes observed during (a) first oxidation and (b) first reduction of **3** in DCB containing 0.2 M (TBA)ClO_4. (c) Spectrum deduced for the charge separation state using spectroelectrochemical data (see text for details, and Figure S20 in SI for complete results). (d) Energy level diagram showing possible charge transfer and charge separation events upon photoexcitation of the compounds **2-4**. NND without linked TCBD in **2-3** is not shown in the abbreviated formula for simplicity.

View Article Online
DOI: 10.1039/D0SC04648E

An energy diagram was established to visualize the energetics of charge transfer and charge separation states in these conjugates, as shown in Figure 4d. Energy of different states were established from free-energy calculations,[58-59] as listed in Table 1. From such a diagram, it was clear that excitation of the conjugates, **2-4** either that the locally excited (near-UV) or charge transfer (visible) peak positions would produce the respective excited states. The excited state species, $(NND\text{-}TCBD)_{1\text{-}3}$-$^{1}TPA^{*}$ formed from the locally excited state would readily produce initial charge transfer state, $(NND\text{-}TCBD)_{1\text{-}3}^{\delta-}$-$TPA^{\delta+}$ involving one of the NND-TCBD entities (free NND is not abbreviated for simplicity). Such a state can also be produced by direct excitation of the visible charge transfer band. The charge transfer state thus generated could further undergo electron transfer to generate the $(NND\text{-}TCBD_{1\text{-}3})^{\cdot-}$-$TPA^{\cdot+}$ charge separated species. Although initial charge separation state would involve only one of the NND-TCBD entities, due to electron exchange, the anion radical could spread over other NND-TCBD entities, as suggested by the earlier discussed frontier LUMOs. Finally, the charge separated species could relax back to the ground state.

In order to probe the anticipated photochemical events and to seek the effect of multiple NND-TCBD entities in prolonging lifetime of charge separated states via the earlier discussed electron exchange mechanism, femtosecond transient absorption studies (fs-TA) were performed. Three solvents of varying polarity were used as the solvent polarity would influence lifetime of charge separated states, and samples were excited at both locally excited (350 nm) and charge transfer (500 nm) peak positions.

As shown in Figure 5a(i), singlet excited state of compound **1** ($^{1}TPA^{*}$) in benzonitrile was formed instantaneously upon 350 nm laser excitation featuring excited state absorption (ESA) maxima at 533, 601 and 1382 nm (see spectrum at 2.22 ps) as well as ground state bleach in 400-450 nm range. To gather insight into the deactivation, global target analysis [60-61] was performed. A kinetic model including three species was satisfactory. The species associated spectra (SAS) and population kinetics of the three species is shown in Figure 5a, ii and iii, respectively. The first species with a lifetime of ~200 fs was within the temporal resolution of our instrument that decayed to develop the second component with singlet excited state features with a lifetime of 49 ps. The third component which could be attributed to the decaying singlet to triplet state had a time constant of about 2.30 ns. Due to lack of any TCBD entities in **1**, no electron transfer could be detected.

View Article Online
DOI: 10.1039/D0SC04648E

In contrast to the spectral features of compound **1**, the donor-acceptor conjugates **2-4** revealed the anticipated ultrafast charge transfer and charge separation processes. In the case of **2**, where only one NND-TCBD entity is present, occurrence of relatively simple photoinduced

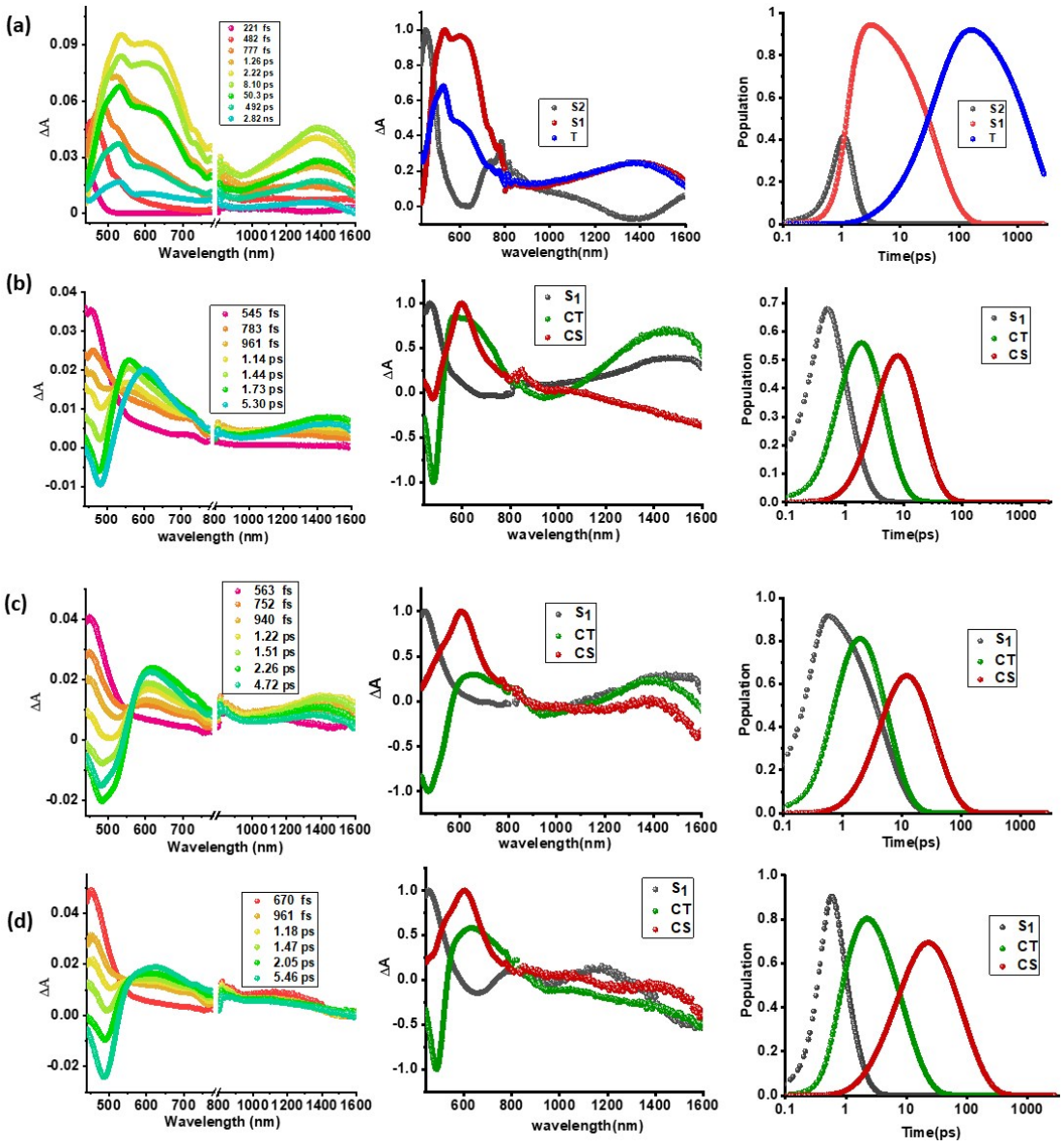

Figure 5. Fs-TA spectra at the indicated delay times, (a-d, panel i), species associated spectra (a-d, panel ii), and population kinetics (a-d, panel iii) of compounds **1-4** (a through d) in benzonitrile. The samples were excited at 350 nm corresponding to locally excited state.

charge transfer could be envisioned. However, in the case of **3** and **4** featuring two and three entities of NND-TCBD attached to TPA, a symmetry breaking charge transfer could be envisioned

View Article Online
DOI: 10.1039/D0SC04648E

due to presence of multiple numbers of equally positioned acceptor entities. Presence of higher number of acceptors could improve the charge transfer by the respective statistical factor or even more by quantum coherence effects.[62] The first panel in Figure 5b-d show transient spectra at the indicated delay times for compounds **2-4**. The ESA peak of the singlet excited state located in the 450-500 nm range revealed rapid decay with a new peaks in the 610-620 nm range and near-IR reange. These spectra were subjected to target analysis that required three components for satisfactory fit. These SAS are shown in Figure 5b-d, middle panel. In all these, the first spectrum with characteristic features of the singlet excited state had a time constant of less than 1 ps, and as predicted, the magnitude of these time constants further decreased with increase in the number of NND-TCBD entities (statistical factor of quenching). The second SAS with time constants of 3.48-5.64 ps has been attributed to the charge transfer state. Here, the depleted peak intensity in the near-IR region has been tentatively assigned to stimulated emission of CT state. With the decay of the second component, the third component was evolved that has been attributed to the charge separated species as this spectrum resembled largely that derived for charge separation product from the earlier discussed spectroelectrochemical studies (see Figure 4c). It may be mentioned here that the SAS of third component is distinctly different from the triplet state SAS shown in Figure 5a, panel ii. The time constants for the charge separated state were found to be 14.9, 32.68 and 75.1 ps, respectively, for compounds **2**, **3**, and **4**. These results reveal persistence of the charge separated state in compounds **3** and **4** compared to that in **2.**

Intrigued with these findings, next, we changed the solvent to less polar DCB and nonpolar toluene. In both of these solvents the spectral trends were almost the same (see Figures S21 and S22 in SI). Further, target analysis was performed to evaluate the kinetic factors as listed in Table 2. Such data confirmed persistence of charge separated states in both solvents. Changing the excitation wavelength to 500 nm corresponding to the charge transfer also revealed excited state charge separation (Figure 6 and Figures S23 and S24). In this case, the data could be satisfactorily fitted to two components, one to the excited state charge transfer with time constants of few ps and the second one for the charge separated state. It may be mentioned here that irrespective of the excitation wavelengths (LE or CT), the SAS generated for charge transfer and charge separation states revealed close resemblance.

View Article Online
DOI: 10.1039/D0SC04648E

Table 2. Time constants evaluated from GloTarAn target analysis of fs-TA spectral data in solvents of varying polarity and at different excitation wavelengths for the investigated central triphenylamine derived, dimethylamine-tetracyanobutadiene conjugates.

Compound	Solvent	λ_{ex}, nm	S_1, ps	CT, ps	CS, ps
1	Toluene	350	842	--	--
2			2.36	4.17	17.02
3			1.56	10.01	39.32
4			0.54	25.37	93.20
2		500	--	3.59	14.92
3			--	7.29	24.10
4			--	16.8	56.30
1	DCB	350	111	--	--
2			1.99	3.87	16.40
3			1.14	8.12	37.59
4			0.35	13.6	87.70
2		500	--	2.49	13.93
3			--	5.78	20.45
4			--	8.76	60.41
1	PhCN	350	49	--	--
2			0.89	3.48	14.9
3			0.80	4.99	32.68
4			0.67	5.64	75.10
2		500	--	1.38	10.23
3			--	3.69	24.65
4			--	4.98	43.29

As pointed out earlier, in synthetic multimodular donor-acceptor systems, charge stabilization is often achieved by following the mechanism of natural photosynthesis where electron migration occurs across the system distantly separating the positive and negative ions thus minimizing their electrostatic attraction.[20-22] Electron/hole delocalization in multiple donor or accepting bearing systems, and utilization of high-energy triplet sensitizers to promote electron transfer from the long-lived triplet excited states are also some of the known mechanisms to extend the lifetime of the charge separated species. The present multi-modular systems, **3** and **4**, differ in their design wherein the same acceptor unit, NND-TCBD is covalently linked to the central TPA. Electron exchange has been witnessed upon first reduction of these compounds unlike that in **2** bearing a single NND-TCBD entity. It appears that such electron exchange is responsible for extending the lifetime of the charge separated states in these novel donor-acceptor conjugates.

View Article Online
DOI: 10.1039/D0SC04648E

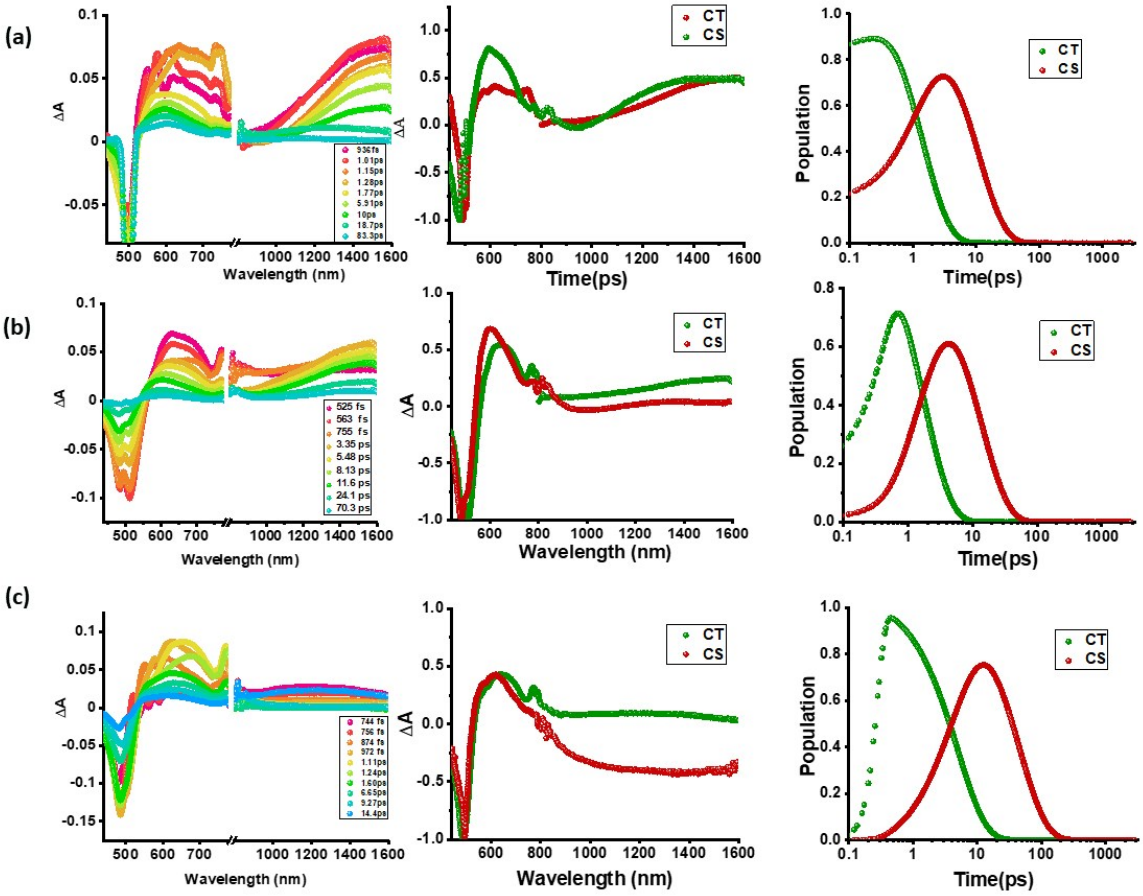

Figure 6. Fs-TA spectra at the indicated delay times of compounds **2-4** in benzonitrile. The samples were excited at 500 nm corresponding to charge transfer band. Right hand panel shows the population kinetics. The dip at 500 nm is due to excitation laser.

Conclusions

In summary, we have developed exceptional molecular donor-acceptor systems consisting of C_3 symmetric central triphenylamine derived, dimethylamine-tetracyanobutadiene conjugates. In these systems, the NND-TCBD promoted charge transfer extending the absorption covering the visible region. Electrochemical studies revealed electron exchange in compounds **3** and **4** carrying multiple numbers of NND-TCBD entities. Frontier LUMO energy levels and orbital coefficients helped us in rationalizing such electron exchange. The spectrum of the charge transfer state was possible to deduce from manipulation of spectroelectrochemical data. Finally, we have been able to demonstrate the effect of electron exchange in prolonging the lifetime of charge separated states

View Article Online
DOI: 10.1039/D0SC04648E

in compounds **3** and **4** from fs-TA spectral studies in solvents of varying polarity. To our knowledge, this is the first report where such a charge stabilizing mechanism involving electron exchange has been proposed and demonstrated experimentally. The present findings are very important to further our understanding on the fundamentals of electron transfer in multi-modular systems; strengthen our knowledge on the early events of natural photosynthesis, and seek novel applications in optoelectronics. In this context, it may be pointed out here that in bacterial photosynthesis, the primary electron donor is an electronically interacting bacteriochlorophyll dimer, $[BChl]_2$.[63] The initial electron transfer species, $[BChl]_2^{\cdot+}$ could slow down the charge recombination via a similar electron exchange mechanism and could be a reason for natural choice of a bacteriochlorophyll dimer instead of a monomer.

Electronic Supplemental Information. Experimental and synthetic details, ^1H and ^{13}C NMR and MALDI-mass of synthesized compounds. Additional CVs, spectroelectrochemical and fs-TA spectral data. Coordinates of optimized geometries.

Conflict of Interest. There are no conflicts to declare.

Acknowledgements. This research was supported by the US-National Science Foundation (2000988 to FD), Council of Scientific and Industrial Research (Project No. CSIR 01(2934)/18/EMR-II), New Delhi and SERB (Project No. CRG/2018/000032) New Delhi, Govt. of India. We gratefully acknowledge Sophisticated Instrumentation Centre (SIC), IIT Indore. IY is thankful to CSIR, India for a research fellowship.

Notes and References

1. N. Armaroli and V. Balzani, *Angewandte Chemie International Edition*, 2007, **46**, 52-66.
2. P. M. Beaujuge and J. M. J. Fréchet, *J. Am. Chem. Soc.*, 2011, **133**, 20009-20029.
3. F. D'Souza and O. Ito, *Chem. Soc. Rev.*, 2012, **41**, 86-96.
4. M. E. El-Khouly, S. Fukuzumi and F. D'Souza, *Chemphyschem*, 2014, **15**, 30-47.
5. Bottari and T. Torres, *"Organic Nanomaterials: Synthesis, Characterization, and Device Applications", Eds: T. Torres and G. Bottari, John Wiley & Sons, Inc., Hoboken, NJ, 2013.*
6. H. Imahori, T. Umeyama and S. Ito, *Acc. Chem. Res.*, 2009, **42**, 1809-1818.
7. D. Gust, T. A. Moore and A. L. Moore, *Faraday Discuss.*, 2012, **155**, 9-26.
8. N. Martín, L. Sánchez, M. Á Herranz, B. Illescas and D. M. Guldi, *Acc. Chem. Res.*, 2007, **40**, 1015-1024

View Article Online
DOI: 10.1039/D0SC04648E

9. G. Bottari, G. de la Torre, D. M. Guldi and T. Torres, *Chem. Rev.*, 2010, **110**, 6768-6816.
10. N. Zarrabi, S. Seetharaman, S. Chaudhuri, N. Holzer, V. S. Batista, A. van der Est, F. D'Souza and P. K. Poddutoori, *J. Am. Chem. Soc.*, 2020, **142**, 10008-10024.
11. L. Hammarström, *Acc. Chem. Res.*, 2015, **48**, 840-850.
12. A. Arrigo, A. Santoro, F. Puntoriero, P. P. Laine and S. Campagna, *Coord. Chem. Rev.*, 2015, **304**, 109-116.
13. S. Fukuzumi, K. Ohkubo and T. Suenobu, *Acc. Chem. Res.*, 2014, **47**, 1455-1464.
14. D. Gust, T. A. Moore and A. L. Moore, *Acc. Chem. Res.*, 2009, **42**, 1890-1898.
15. F. D'Souza and O. Ito, *Chem. Soc. Rev.*, 2012, **41**, 86-96.
16. M. Barrejón, L. M. Arellano, F. D'Souza and F. Langa, *Nanoscale*, 2019, **11**, 14978-14992.
17. C. B. KC and F. D'Souza, *Coord. Chem. Rev.*, 2016, **322**, 104-141.
18. D. Kim, *Multiporphyrin arrays: Fundamentals and applications*, 2012.
19. R. Canton-Vitoria, H. B. Gobeze, V. M. Blas-Ferrando, J. Ortiz, Y. Jang, F. Fernández-Lázaro, Á Sastre-Santos, Y. Nakanishi, H. Shinohara, F. D'Souza and N. Tagmatarchis, *Angew. Chem. Int. Ed. Engl.*, 2019, **58**, 5712-5717.
20. R. Cogdell and C. Mullineaux, *Photosynthesis Res.*, 2008, **95**, 117.
21. R. C. Leegood, *Annals of Botany*, 2006, **97**, 152-153.
22. B. Green and W. W. Parson, *Light-Harvesting Antennas in Photosynthesis*, Springer Netherlands, 2003.
23. T. Hasobe, P. V. Kamat, V. Troiani, N. Solladié, T. K. Ahn, S. K. Kim, D. Kim, A. Kongkanand, S. Kuwabata and S. Fukuzumi, *J Phys Chem B*, 2005, **109**, 19-23.
24. T. Hasobe, K. Saito, P. V. Kamat, V. Troiani, H. Qiu, N. Solladié, K. S. Kim, J. K. Park, D. Kim, F. D'Souza and S. Fukuzumi, *J. Mater. Chem.*, 2007, **17**, 4160-4170.
25. C. Obondi O., G. N. Lim, B. Churchill, P. K. Poddutoori, A. van der Est and F. D'Souza, *Nanoscale*, 2016, **8**, 8333-8344.
26. D. R. Subedi, H. B. Gobeze, Y. E. Kandrashkin, P. K. Poddutoori, A. van der Est and F. D'Souza, *Chem. Commun.*, 2020, **56**, 6058-6061.
27. S. Gangala and R. Misra, *J. Mater. Chem. A*, 2018, **6**, 18750-18765.
28. A. Hagfeldt, G. Boschloo, L. Sun, L. Kloo and H. Pettersson, *Chem. Rev.*, 2010, **110**, 6595-6663.
29. L. Sun, F. Bai, Z. Zhao and H. Zhang, *Solar Energy Mater. Solar Cells*, 2011, **95**, 1800-1810.

View Article Online
DOI: 10.1039/D0SC04648E

30. Y. Patil and R. Misra, *Chem. Asian J.*, 2018, **13**, 220-229.
31. Y. Wu and W. Zhu, *Chem. Soc. Rev.*, 2013, **42**, 2039-2058.
32. M. Y. Berezin and S. Achilefu, *Chem. Rev.*, 2010, **110**, 2641-2684.
33. J. Min, Y. N. Luponosov, D. Baran, S. N. Chvalun, M. A. Shcherbina, A. V. Bakirov, P. V. Dmitryakov, S. M. Peregudova, N. Kausch-Busies, S. A. Ponomarenko, T. Ameri and C. J. Brabec, *J. Mater. Chem. A*, 2014, **2**, 16135-16147.
34. F. Bures, W. B. Schweizer, J. C. May, C. Boudon, J. Gisselbrecht, M. Gross, I. Biaggio and F. Diederich, *Chemistry*, 2007, **13**, 5378-5387.
35. J. Wang, Q. Xiao and J. Pei, *Org. Lett.*, 2010, **12**, 4164-4167.
36. M. Poddar and R. Misra, *Chem. Asian J.*, 2017, **12**, 2908-2915.
37. Y. Patil, R. Misra, F. C. Chen, M. L. Keshtov and G. D. Sharma, *RSC Adv.*, 2016, **6**, 99685-99694.
38. T. Ishi-i, K. Ikeda, M. Ogawa and Y. Kusakaki, *RSC Adv.*, 2015, **5**, 89171-89187.
39. Y. Li, S. Gao, N. Zhang, X. Huang, J. Tian, F. Xu, Z. Sun, S. Yin, X. Wu and W. Chu, *J. Mater. Chem. C*, 2019, **7**, 2686-2698.
40. A. Kundu, S. Karthikeyan, D. Moon and S. P. Anthony, *CrystEngComm*, 2017, **19**, 6979-6985.
41. M. Kivala, C. Boudon, J. Gisselbrecht, P. Seiler, M. Gross and F. Diederich, *Angew. Chem. Int. Ed.*, 2007, **46**, 6357-6360.
42. A. Gopinath, N. Manivannan, S. Mandal, N. Mathivanan and A. S. Nasar, *J. Mater. Chem. B*, 2019, **7**, 6010-6023.
43. T. Michinobu, C. Boudon, J. Gisselbrecht, P. Seiler, B. Frank, N. N. P. Moonen, M. Gross and F. Diederich, *Chemistry – A European Journal*, 2006, **12**, 1889-1905.
44. M. Kivala, C. Boudon, J. Gisselbrecht, P. Seiler, M. Gross and F. Diederich, *Angew. Chem. Int. Ed.*, 2007, **46**, 6357-6360.
45. T. Michinobu, *Chem. Soc. Rev.*, 2011, **40**, 2306-2316.
46. T. Shoji, S. Ito, K. Toyota, T. Iwamoto, M. Yasunami and N. Morita, *Eur. J. Org. Chem.*, 2009, **2009**, 4307-4315.
47. P. Gautam, R. Sharma, R. Misra, M. L. Keshtov, S. A. Kuklin and G. D. Sharma, *Chem. Sci.*, 2017, **8**, 2017-2024.
48. Y. Patil, R. Misra, R. Singhal and G. D. Sharma, *J. Mater. Chem. A*, 2017, **5**, 13625-13633.

View Article Online
DOI: 10.1039/D0SC04648E

49. M. Sekita, B. Ballesteros, F. Diederich, D. M. Guldi, G. Bottari and T. Torres, *Angew. Chem. Int. Ed.*, 2016, **55**, 5560-5564.
50. K. A. Winterfeld, G. Lavarda, J. Guilleme, M. Sekita, D. M. Guldi, T. Torres and G. Bottari, *J. Am. Chem. Soc.*, 2017, **139**, 5520-5529.
51. K. A. Winterfeld, G. Lavarda, J. Guilleme, D. M. Guldi, T. Torres and G. Bottari, *Chem. Sci.*, 2019, **10**, 10997-11005.
52. H. Gotfredsen, T. Neumann, F. E. Storm, A. V. Muñoz, M. Jevric, O. Hammerich, K. V. Mikkelsen, M. Freitag, G. Boschloo and M. B. Nielsen, *ChemPhotoChem*, 2018, **2**, 976-985.
53. P. Gautam, R. Misra, M. B. Thomas and F. D'Souza, *Chem. Eur. J.*, 2017, **23**, 9192-9200.
54. R. Sharma, M. B. Thomas, R. Misra and F. D'Souza, *Angew. Chem. Int. Ed.*, 2019, **58**, 4350-4355.
55. Y. Rout, Y. Jang, H. B. Gobeze, R. Misra and F. D'Souza, *J. Phys. Chem. C*, 2019, **123**, 23382-23389.
56. M. Poddar, Y. Jang, R. Misra and F. D'Souza, *Chem. Eur. J.*, 2020, **26**, 6869-6878.
57. *Gaussian 09*, Revision C.01, M. J. Frisch, G. W. Trucks, H. B. Schlegel, G. E. Scuseria, M. A. Robb, J. R. Cheeseman, G. Scalmani, V. Barone, B. Mennucci, G. A. Petersson, H. Nakatsuji, M. Caricato, X. Li, H. P. Hratchian, A. F. Izmaylov, J. Bloino, G. Zheng, J. L. Sonnenberg, M. Hada, M. Ehara, K. Toyota, R. Fukuda, J. Hasegawa, M. Ishida, T. Nakajima, Y. Honda, O. Kitao, H. Nakai, T. Vreven, J. A. , Jr. , Montgomery, J. E. Peralta, F. Ogliaro, M. Bearpark, J. J. Heyd, E. Brothers, K. N. Kudin, V. N. Staroverov, R. Kobayashi, J. Normand, K. Raghavachari, A. Rendell, J. C. Burant, S. S. Iyengar, J. Tomasi, M. Cossi, N. Rega, J. M. Millam, M. Klene, J. E. Knox, J. B. Cross, V. Bakken, C. Adamo, J. Jaramillo, R. Gomperts, R. E. Stratmann, O. Yazyev, A. J. Austin, R. Cammi, C. Pomelli, J. W. Ochterski, R. L. Martin, K. Morokuma, V. G. Zakrzewski, G. A. Voth, P. Salvador, J. J. Dannenberg, S. Dapprich, A. D. Daniels, Ö. Farkas, J. B. Foresman, J. V. Ortiz, J. Cioslowski, D. J. Fox, Gaussian, Inc., Wallingford, CT, USA, **2009**.
58. D. Rehm and A. Weller, *Isr. J. Chem.*, 1970, **8**, 259-271.
59. Gibbs free-energy change associated for excited state charge separation (CS) and dark charge recombination (CR) were estimated according to equations i-iii

$$-\Delta G_{CR} = E_{ox} - E_{red} + \Delta G_S \quad \text{(i)}$$

$$-\Delta G_{CS} = \Delta E_{00} - (-\Delta G_{CR}) \quad \text{(ii)}$$

View Article Online
DOI: 10.1039/D0SC04648E

where ΔE_{00} corresponds to the singlet state energy of 1. The term ΔG_S refers to electrostatic energy calculated according to dielectric continuum model (see equation iii). The E_{ox} and E_{red} represent the oxidation potential and the first reduction potential, respectively.

$$\Delta G_S = e^2/4\ \pi\ \varepsilon_o\ [\ -\ 1/R_{cc}\ \varepsilon_R) \qquad \text{(iii)}$$

The symbols ε_0 and ε_R represent vacuum permittivity and dielectric constant of DCB used for photochemical and electrochemical studies (= 9.93). R_{CC} are the center-to-center distance between donor and acceptor entities from the computed structures. Energy of charge transfer was calculated from peak maxima of charge transfer peak.

60. J. Snellenburg, S. Laptenok, R. Seger, K. Mullen,and I. van Stokkum, *J. of Stat. Software*, 2012, **49** 1-22.
61. http://glotaran.org/
62. S. Rafiq and G. D. Scholes, *J. Am. Chem. Soc.*, 2019, **141**, 708-722.
63. J. Deisenhofer, O. Epp, K. Miki, R. Huber and H. Michel, *J. Mol. Biol.*, 1984, **180**, 385-398.

View Article Online
DOI: 10.1039/D0SC04648E

Table of content

Charge Stabilization via Electron Exchange: Excited Charge Separation in Symmetric, Central Triphenylamine Derived, Dimethylaminophenyl-Tetracyanobutadiene Donor-Acceptor Conjugates

I. S. Yadav, A. Z. Alsaleh, R. Misra and F. D'Souza**

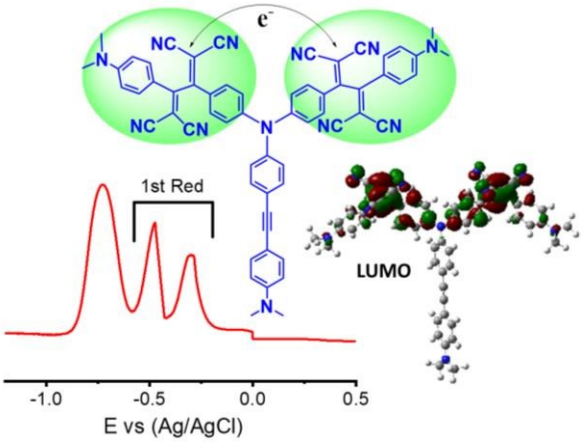

Significance of electron exchange in stabilizing the charge-separated state is revealed in multi-modular donor-acceptor conjugates.